

Effect of Hall current on the MHD laminar natural convection flow from a vertical permeable flat plate with uniform surface temperature

L.K. Saha^a, M.A. Hossain^{b,*}, Rama Subba Reddy Gorla^c

^a Department of Mathematics, University of Dhaka, Dhaka 1000, Bangladesh

^b Department of Mathematics, COMSATS Institute of Information and Technology, Islamabad, Pakistan

^c Department of Mechanical Engineering, Cleveland State University, Ohio, USA 44 115

Received 2 February 2006; received in revised form 2 October 2006; accepted 11 October 2006

Available online 4 December 2006

Abstract

The effect of Hall current on the steady, laminar, natural convection boundary layer flow of MHD viscous and incompressible fluid from a semi-infinite heated permeable vertical flat plate with an applied magnetic field transverse to it has been investigated, assuming that the induced magnetic field is negligible compared to the imposed magnetic field. With appropriate transformations the boundary layer equations are reduced to local nonsimilarity equations and the solutions are obtained employing four distinct methods, namely, (i) regular perturbation method for small transpiration parameter; (ii) asymptotic solutions for large transpiration rate; (iii) implicit finite difference method together with Keller-box scheme and the (iv) local nonsimilarity method for any transpiration rate. Effects of the magnetic field, M , and the Hall parameter, m , on the local skin friction and local rate of heat transfer groups are shown graphically for smaller values of the Prandtl number, $Pr (= 0.1, 0.01)$, that represent liquid metals.

© 2006 Elsevier Masson SAS. All rights reserved.

Keywords: Natural convection; Hall current effects; Magnetohydrodynamics; Boundary level

1. Introduction

Magnetohydrodynamics can be regarded as a combination of fluid mechanics and electro-magnetism, that is, the behaviour of electrically conducting fluid in the presence of magnetic and electric fields. The study of magnetohydrodynamic natural convection flow and heat transfer of an electrically conducting fluid past a heated semi-infinite vertical porous plate finds useful applications in many engineering problems such as MHD generator, Plasma studies, nuclear reactors, geothermal extractions and the boundary layer control in the field of aeronautics and aerodynamics. It serves as the basis for understanding some of the important phenomena occurring in heat exchanger devices.

The natural convection boundary layer flow of an electrically conducting fluid up a hot vertical plate in presence of strong magnetic field has been discussed by several authors, such as Singh and Cowling [1], Sparrow and Cess [2], Gupta [3], Riley [4], Kuiken [5], Wilks [6]. Singh and Cowling have shown that regardless of the strength of the applied magnetic field there will always be a region in the neighborhood of the leading edge of the plate where electromagnetic force are unimportant, whilst at large distances from the leading edge this magnetic force dominate. The flow near the leading edge has been examined by Sparrow and Cess [2] whilst Singh and Cowling [1] focused their attention on conditions at downstream. In particular they concentrated on examining that outer region of the boundary layer, which must always ultimately appertain, in which an inviscid balance between buoyancy and magnetic forces is achieved. Subsequent authors, Riley and Kuiken [5] have re-examined the problem with a view to incorporating in the solution the inner viscous layer within the downstream boundary layer which is appropriate if the boundary condition of ‘no-slip’ at the plate is to be satisfied. In Wilks [6] work, it

* Corresponding author.

E-mail addresses: lksaha_math@yahoo.com (L.K. Saha), anwar@univdhaka.edu (M.A. Hossain), r.gorla@csuohio.edu (R.S.R. Gorla).

¹ On leave of absence from the Department of Mathematics, University of Dhaka, Dhaka 1000, Bangladesh.

Nomenclature

B	magnetic induction
C_{fx}	local skin friction
e	electronic charge
E	intensity of electric field
g	gravitational acceleration
Gr_x	modified Grashof number
H	magnetic intensity
J	electric current density
m	Hall parameter
M	magnetic parameter
Nu_x	local Nusselt number
p	pressure
Pr	Prandtl number
T	temperature of the fluid
T_∞	free stream temperature
x, y, z	co-ordinate directions
u, v, w	velocity components in x, y, z directions
v	velocity component normal to u

V	transpiration velocity
x	axial coordinate
y	coordinate normal to x

Greek letters

α	thermal diffusivity
β	volumetric expansion coefficient for temperature
ψ	stream function
θ	dimensionless temperature function
ρ	density
ν	kinematic viscosity
μ	dynamic viscosity
ζ	transpiration parameter
η	pseudo similarity variable

Subscripts

w	conditions at wall
∞	conditions far away from wall

was illustrated that the problem may be formulated in terms of regular and inverse series expansions of a characterizing coordinate that essentially provide a link between the similarity states appropriate to the leading edge and the downstream region. Hossain et al. [7] have investigated the MHD free convection and mixed convection flow along a vertical porous flat plate with a power law surface temperature in the presence of variable transverse magnetic field. The problem of free convection flow from an inclined surface to the horizontal has been investigated by Hossain et al. [8]. Hossain [9] studied the effect of viscous and Joules heating on the flow of an electrically conducting fluid past a semi-infinite plate of which temperature varies linearly with the distance from the leading edge in the presence of uniform transverse magnetic field. Conjugate effects of heat and mass transfer on the flow along a vertical plate in the presence of the transverse magnetic field have been investigated by Elbashbeshy [10].

Suction and injection of a different gas has a great importance in controlling the boundary-layer thickness and the rate of heat transfer has motivated many researchers to investigate its effects on forced and free convection flows. Similarity solutions of the problem were given by Eichhorn [11], who considered power law variations in the plate temperature and transpiration velocity. Constant plate temperature and transpiration velocity were discussed by Sparrow and Cess [12]. They obtained series expansions for temperature and velocity distributions in powers of $x^{1/2}$, where x represents the distance in the stream-wise direction measured from the leading edge. Merkin presented numerical solutions for free convection heat transfer with blowing along an isothermal vertical flat plate [13,14] and Perikh et al. [15]. Both Hartnett–Eckert [16] and Sparrow–Starr [17] reported the characteristics of heat transfer and skin friction for pure forced convection with blowing, while the former dealt with a nonsimilar case. Locally nonsimilar solutions

for convection flow with arbitrary transpiration velocity were obtained by Kao [18,19] applying Görtler–Meksin transformations. Free convection flow along a vertical plate with arbitrary blowing and wall temperature has also been investigated by Vedhanayagam et al. [20]. The free convection flow over a horizontal plate was investigated by Lin and Wu [21], who considered temperature and transpiration rates, which both followed power-law variations. Hossain et al. [8,22] investigated the natural convection flow from a vertical permeable flat plate with variable surface temperature, considering temperature and transpiration rates which both followed power-law variations. Steady free convection flow of an electrically conducting fluid under the transverse magnetic field past a semi-infinite vertical porous plate was analyzed by Cobble [23]. He derived the conditions to be satisfied by the magnetic field for the existence of a similarity solution when the plate temperature is assumed to vary with x , where x is measured from the leading edge of the plate. Soundalgekar et al. [24] investigated the same problem, taking into account the variable plate temperature and with suction and injection.

When the conducting fluid is an ionized gas, and the strength of the applied magnetic field is large, the conductivity normal to the magnetic field is reduced due to the free spiraling of electrons and ions about the magnetic lines of force before suffering collisions and a current is induced in a direction normal to both electric and magnetic field. This phenomenon is called Hall effect. In all of the above investigations, the effects of Hall current have not been considered. When the medium is rarefied or if a strong magnetic field is present, the conductivity of the fluid is anisotropic and the effect of Hall current cannot be neglected.

The study of MHD viscous flows with Hall current has important applications in problems of Hall accelerators as well as flight magnetohydrodynamics. The current trend for the application of magneto hydrodynamics is toward a strong magnetic

field (so that the influence of electromagnetic force is noticeable) and towards a low density of the gas (such as in space flight and in nuclear fusion research). Under this condition the Hall current and ion slip become important.

With the above understanding, Sato [25], Yamanishi [26], Sherman and Sutton [27] studied the hydrodynamic flow of a viscous liquid through straight channel taking Hall effects into account. With regards to external hydrodynamic flows, Katagiri [28] discussed the effect of Hall current on the boundary layer flow past a semi-infinite plate. Gupta [29], Datta and Mazumder [30] and Pop and Soundalgekar [31] investigated the Hall effects in the steady hydrodynamic flow past an infinite porous plate. All of above authors considered one-dimensional flow. Pop and Watanabe [32] presented the problem of free convection flow of a conducting fluid is permeated by a transverse magnetic field and the Hall effect are taken into account. Aboeldahab and Elbarbary [33] took into account the effect of Hall current on the magnetohydrodynamic free-convection flow in presence of foreign species over a vertical surface upon which the flow is subjected to a strong external magnetic field.

The purpose of the present investigation is to study the effect of Hall current on the magnetohydrodynamic natural convection boundary layer flow past a semi-infinite vertical permeable flat plate with a uniform mass flux, since it has important application in space flight and in nuclear fusion. The transformed boundary-layer equations are solved numerically near to and far from the leading edge, using perturbation method appropriate to small and large transpiration parameter $\zeta (= (V_0 x / \nu) / Gr_x^{1/4})$. Solutions for intermediate locations are also obtained using the Keller-box technique (Keller [34]) as well as by the local non-similarity method developed by Minkowycz and Sparrow [35]. The effects of the major parameters such as M , m for smaller values of the Prandtl number $Pr (= 0.1$ and 0.01 , appropriate to liquid metals which currently used in nuclear engineering used as coolant. For example, value of Prandtl number, for lithium and mercury found to be 0.05 and 0.01 , respectively) on the local skin-friction coefficient and local Nusselt number at the surface are discussed in detail. Also representative results for the velocity and temperature distributions are presented for various values of transpiration parameter, ζ .

2. Formulation of the problem

Consider the steady natural convection boundary layer flow of an electrically conducting and viscous incompressible fluid from a semi-infinite heated permeable vertical flat plate in presence of a transverse magnetic field with the effect of Hall currents. The x -axis is along the vertically upward direction while the y -axis is normal to it and away from the plate surface. The leading edge of the permeable surface is taken as coincident with z -axis. The plate temperature is assumed to be nonuniform and depending on the distance x measured from the leading edge of the plate whereas the ambient temperature maintained at uniform temperature, T_∞ . Further we consider a uniform mass flux, V_0 through the permeable vertical surface of the plate. The flow configuration and the coordinate system are shown in Fig. 1. The effect of Hall currents gives rise to a

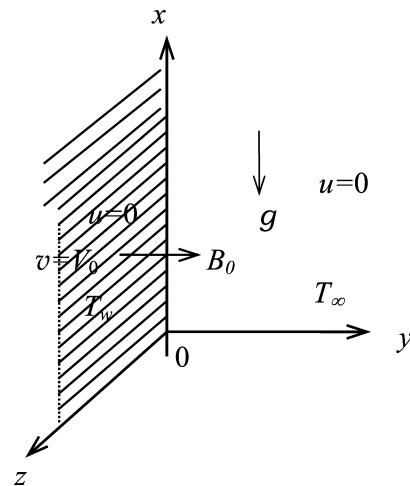


Fig. 1. The flow configuration and the coordinate system.

force in that direction and hence, the flow becomes to be three-dimensional. To simplify the problem, we assume that there is no variation of flow quantities in z -direction. This assumption is considered to be valid if the surface be of infinite extent in the z -direction. Although the pattern of electric currents in the extremities in the z -direction is considered to be unrealizable under the assumption, it might be expected to give an insight into the behaviour of Hall current on the flow.

The fundamental equations for steady incompressible magnetohydrodynamic flows with generalized Ohm's law and Maxwell's equations under the assumption that the fluid is quasi-neutral and ion slip and thermoelectric effect can be neglected are as follows:

Continuity equation:

$$\nabla \cdot V = 0 \quad (1)$$

Momentum equation:

$$(V \cdot \nabla)V = -\frac{1}{\rho} \nabla p + \nu \nabla^2 V + \frac{1}{\rho} J \times B + g\beta(T - T_\infty) \quad (2)$$

Energy equation:

$$(V \cdot \nabla)T = \alpha \nabla^2 T \quad (3)$$

Ohm's law:

$$J = \sigma \left(E + V \times B - \frac{1}{en_e} J \times B + \frac{1}{en_e} \nabla p_e \right) \quad (4)$$

Maxwell's equation:

$$\nabla \times H = J, \quad \nabla \times E = 0, \quad \nabla \cdot B = 0 \quad (5)$$

where V is the velocity vector, p is the pressure, J is the electric current density, B is the magnetic induction vector, which has connection with the magnetic intensity H and the magnetic permeability μ_e as $\mu_e H$, E is the intensity of the electric field, p_e the electronic pressure, e the electric charge, n_e the number of density of electron, ρ the density of the fluid, ν the kinematic coefficient of viscosity, g the acceleration due to gravity, β the coefficient of thermal expansion and T_∞ is the ambient temperature.

From (5), using the relation $\nabla \cdot B = 0$ for the magnetic field $B = (B_x, B_y, B_z)$ we obtain that $B_y = B_0$ (may be constant or variable) everywhere in fluid. This assumption is valid only when the magnetic Reynolds number is very small. For the current density $J = (J_x, J_y, J_z)$ we obtain from the relation $\nabla \cdot J = 0$ that $J_y = \text{constant}$. Hence we consider that the plate is nonconducting and therefore $J_y = 0$ at the plate and hence zero everywhere. Finally we consider the case of a short circuit problem in which the applied electric field $E = 0$. Further by the assumption of small magnetic Reynolds number, an induced magnetic field can be neglected in comparison with the applied magnetic field B_0 . In addition, we assume the fluid is isotropic and homogeneous and has the scalar constant viscosity and electric conductivity. Under the usual boundary layer approximation, basic equations can be simplified to the following equations:

$$\frac{\partial u}{\partial x} + \frac{\partial v}{\partial y} = 0 \quad (6)$$

$$u \frac{\partial u}{\partial x} + v \frac{\partial u}{\partial y} = \nu \frac{\partial^2 u}{\partial y^2} + g\beta(T - T_\infty) - \frac{B_0}{\rho} J_z \quad (7)$$

$$u \frac{\partial w}{\partial x} + v \frac{\partial w}{\partial y} = \nu \frac{\partial^2 w}{\partial y^2} + \frac{B_0}{\rho} J_x \quad (8)$$

$$u \frac{\partial T}{\partial x} + v \frac{\partial T}{\partial y} = \alpha \frac{\partial^2 T}{\partial y^2} \quad (9)$$

$$J_x = \frac{\sigma B_0}{(1 + m^2)}(mu - w) \quad (10)$$

$$J_z = \frac{\sigma B_0}{(1 + m^2)}(u + mw) \quad (11)$$

Here u, v and w are the x -, y - and z -components of the velocity vector V , the subscript x and z denote, respectively, the x - and z -components of the vectorial quantities. $m(= \omega^2 \tau^2)$ is the Hall parameter, with ω as the cyclotron frequency of electron and τ as collision time of electrons with ions

$$\begin{aligned} u(x, y) &= 0, & v(x, y) &= -V_0, & w(x, y) &= 0 \\ T(x, y) &= T_w & \text{at } y &= 0 \\ u(x, y) &= 0, & w(x, y) &= 0 \\ T(x, y) &= T_\infty & \text{at } y &= \infty \end{aligned} \quad (12)$$

In Eq. (12) V_0 is the transpiration velocity. For withdrawal of fluid through the surface it is positive while for blowing of fluid it is negative. In the present investigation, we have considered the case of withdrawal or suction of fluid through the permeable surface.

To integrate the set of nonlinear partial differential equations (8) to (9) together with the current intensity components described in (11) and (12) we need to transform these to a convenient form. And to do that, we introduce the following dimensionless group of transformations for the dependent and independent variables that are appropriate for the natural convection flow from a vertical surface:

$$\begin{aligned} \psi(x, y) &= \nu Gr_x^{1/4} [f(\zeta, \eta) + \zeta] \\ \eta &= \frac{y}{x} Gr_x^{1/4}, & \zeta &= \frac{V_0 x}{\nu} Gr_x^{-1/4} \\ w(x, y) &= \frac{\nu}{x} Gr_x^{1/2} g(\zeta, \eta) \\ \theta &= \frac{T - T_\infty}{T_w - T_\infty} = \frac{T - T_\infty}{\Delta T} \end{aligned} \quad (13)$$

where ψ is the stream function, defined by

$$u = \frac{\partial \psi}{\partial y} \quad \text{and} \quad v = -\frac{\partial \psi}{\partial x} \quad (14)$$

which satisfies the continuity equation (6). In Eq. (13), f is the dimensionless stream function, g is the dimensionless velocity component in z -direction, θ is the dimensionless temperature of the fluid in the boundary layer, $\Delta T = T_w - T_\infty$, η is the pseudo-similarity variable. ζ is the transpiration parameter depending on the transpiration velocity V_0 as well as the axial variable x , which is positive when fluid is being sucked and negative when fluid is being injected through the permeable surface. This may also be interpreted as being a scaled stream wise variable; since this depends on the axial coordinate x , which is small near the leading edge and large in the downstream regime. Finally Gr_x and M are, respectively, the local Grashof number and the magnetic field number as given below:

$$Gr_x = \frac{g\beta \Delta T}{\nu^2} x^3, \quad M = \frac{\sigma B_0^2 x^2}{\rho Gr_x^{1/2}}$$

Here we have considered that the applied magnetic field component B_0 is proportional to $x^{-1/4}$ that is strong in the region near the leading edge and weak in the downstream regime.

Now, substituting the group of transformations given in (6)–(12) together with (14) one may obtain the following nonsimilarity equations:

$$\begin{aligned} f''' + \frac{3}{4} f f'' - \frac{1}{2} f'^2 + \zeta f'' + \theta - \frac{M}{(1 + m^2)} (f' + mg) \\ = \frac{1}{4} \zeta \left[f' \frac{\partial f'}{\partial \zeta} - f'' \frac{\partial f}{\partial \zeta} \right] \end{aligned} \quad (15)$$

$$\begin{aligned} g'' + \frac{3}{4} f g' - \frac{1}{2} f' g + \zeta g' - \frac{M}{(1 + m^2)} (g - m f') \\ = \frac{1}{4} \zeta \left[f' \frac{\partial g}{\partial \zeta} - g' \frac{\partial f}{\partial \zeta} \right] \end{aligned} \quad (16)$$

$$\frac{1}{Pr} \theta'' + \frac{3}{4} f \theta' + \zeta \theta' = \frac{1}{4} \zeta \left[f' \frac{\partial \theta}{\partial \zeta} - \theta' \frac{\partial f}{\partial \zeta} \right] \quad (17)$$

In Eq. (17) $Pr(= \nu/\alpha)$ is the Prandtl number. In these equations, primes denote differentiation of the functions with respect to η .

The boundary conditions appropriate to the above equations are:

$$\begin{aligned} f(\zeta, 0) = f'(\zeta, 0) = 0, & \quad g(\zeta, 0) = 0, & \quad \theta(\zeta, 0) = 1 \\ f'(\zeta, \infty) = g(\zeta, \infty) = \theta(\zeta, \infty) = 0 \end{aligned} \quad (18)$$

Eqs. (15)–(17) are parabolic partial equations by nature. Once we know the solutions of the above equations, the physical quantities of interest are the skin-friction and the Nusselt

number, which may be calculated from the following expressions:

$$C_{fx} Gr_x^{-3/4} = f''(\zeta, 0), \quad Nu_x Gr_x^{-1/4} = -\theta'(\zeta, 0) \quad (19)$$

In absence of the magnetic field, the present problem, for the flow along a vertical porous surface had been investigated by Merkin [13]. This investigation had been confined to the fluid for which the value of the Prandtl number is unity.

On the other hand, for the case of the natural convection flow from a rigid vertical surface in presence of a transverse magnetic field but in absence of Hall current, the problem had been investigated by Sparrow and Cess [2], for smaller values of the local magnetic field parameter for fluids having the value of the Prandtl number, $Pr = 10.0, 0.72$ and 0.02 using the regular perturbation technique treating the local magnetic field variable as small. Later, the problem posed by Merkin [13] has been investigated by Soundalgekar et al. [24] for the values of axially distributed magnetic field. But, in presence of Hall current the problem on the magneto-hydrodynamic natural convection flow of viscous incompressible fluid with transverse magnetic field for a vertical rigid surface (i.e., nonporous surface) have been studied by Pop and Watanabe [32]. The present authors revisited all the above studies and found excellent agreement with the respective results. Some comparisons will be shown in the discussion.

3. Solution methodologies

In the present investigation we shall integrate Eqs. (15)–(18) for small and large values of the axially distributing transpiration parameter, ζ , employing the regular perturbation method. The implicit finite difference method together with Keller-box elimination technique (Keller [34]) has been applied for entire region of ζ . Solutions of the aforementioned equations are also obtained employing the local nonsimilarity method of Minkowycz and Sparrow [35] for the case of entire regime.

3.1. Regular perturbation solutions (ESS) for small ζ

The series solution is valid for sufficiently small values of ζ , that is, either for sufficiently small distances from the leading edge or for small values of V (see the definition of ζ in Eq. (13). Accordingly the functions $f(\zeta, \eta)$, $g(\zeta, \eta)$ and $\theta(\zeta, \eta)$ expanded in a power series in ζ , that is, we take

$$\begin{aligned} f(\eta, \zeta) &= \sum_{i=0}^{\infty} \zeta^i f_i(\eta) \\ g(\eta, \zeta) &= \sum_{i=0}^{\infty} \zeta^i g_i(\eta) \\ \theta(\eta, \zeta) &= \sum_{i=0}^{\infty} \zeta^i \theta_i(\eta) \end{aligned} \quad (20)$$

On substituting these into Eqs. (9)–(12) and equating the terms of like powers of ζ to zero, the leading order equations are obtained as follows:

$$f_0''' + \frac{3}{4} f_0 f_0'' - \frac{1}{2} f_0'^2 + \theta_0 - \frac{M}{(1+m^2)} (f_0' + m g_0) = 0 \quad (21)$$

$$g_0'' + \frac{3}{4} f_0 g_0' - \frac{1}{2} f_0 g_0 - \frac{M}{(1+m^2)} (g_0 - m f_0') = 0 \quad (22)$$

$$\frac{1}{Pr} \theta_0'' + \frac{3}{4} f_0 \theta_0' = 0 \quad (23)$$

and the boundary conditions are:

$$\begin{aligned} f_0 = f_0' = 0, \quad g_0 = 0, \quad \theta_0 = 1 \quad \text{at } \eta = 0 \\ f_0' \rightarrow 0, \quad g_0 \rightarrow 0, \quad \theta_0 \rightarrow 0 \quad \text{as } \eta \rightarrow \infty \end{aligned} \quad (24)$$

The higher order equations, for $i \geq 1$, are as obtained given below

$$\begin{aligned} f_i''' + f_{i-1}'' + \theta_i - \frac{M}{(1+m^2)} (f_i' + m g_i) \\ = \sum_{r=0}^i \left[\left(\frac{1}{2} + \frac{r}{4} \right) f_r' f_{i-r}' - \left(\frac{3}{4} + \frac{r}{4} \right) f_r f_{i-r}'' \right] \end{aligned} \quad (25)$$

$$\begin{aligned} g_i'' + g_{i-1}' - \frac{M}{(1+m^2)} (g_i - m f_i') \\ = \sum_{r=0}^i \left[\left(\frac{1}{2} + \frac{r}{4} \right) g_r f_{i-r}' - \left(\frac{3}{4} + \frac{r}{4} \right) f_r g_{i-r}' \right] \end{aligned} \quad (26)$$

$$\frac{1}{Pr} \theta_i'' + \theta_{i-1}' = \sum_{r=0}^i \left[\frac{r}{4} g_r f_{i-r}' - \left(\frac{3}{4} + \frac{r}{4} \right) f_r g_{i-r}' \right] \quad (27)$$

In the above f_0 , g_0 and θ_0 are the well-known similarity solutions for free convection flow around a semi-infinite isothermal vertical plate, and the functions f_i , g_i and θ_i ($i = 1, 2, 3, \dots$) are effectively first and higher order corrections to the flow due to the effect of the transpiration of fluid through the surface of the plate. Further, Eqs. (21)–(27) (for each $i \geq 1$) are linear, but coupled, and may be found by pair-wise sequential solution. These pairs of equations have been integrated using an implicit Runge–Kutta–Butcher (Butcher [36]) initial value solver together with the iteration scheme of Nachtsheim and Swigert [37].

The solution of the above equations enables the calculation of various flow parameters near the leading edge, such as the skin-friction, C_{fx} , and Nusselt number, Nu_x . Using the relations given in (19), the quantities C_{fx} and Nu_x can now be calculated respectively from the following expressions:

$$C_{fx} Gr_x^{-3/4} = f''(\zeta, 0) = (f_0'' + \zeta f_1'' + \zeta^2 f_2'' + \dots) \quad (28)$$

$$Nu_x Gr_x^{-1/4} = -\theta'(\zeta, 0) = -(\theta_0' + \zeta \theta_1' + \zeta^2 \theta_2' + \dots) \quad (29)$$

A comparison of the perturbation solution functions f_0'' , f_1'' , θ_0' and θ_1' obtained in the present authors and obtained earlier by Merkin [13] has been shown in Table 1 and found an excellent agreement among the respective results. Solutions obtained by the aforementioned author for the f_0'' and θ_0' may be reproduced simply by dividing and multiplying the present values by the factor $\sqrt{2}$ respectively and f_1'' may be reproduced by dividing the present values by 2, θ_1' remains unchanged.

3.2. Asymptotic solutions (ASS) for large ζ

In this section attention is given to the solution of Eqs. (15)–(18) when ζ is large. The order of magnitude analysis of various terms in (15)–(17) shows that the largest are f''' and $\zeta f''$ in (15), g'' and $\zeta g'$ in (16), and θ'' and $\zeta \theta'$ in (17). In the respective equations both the terms have to be balanced in magnitude and the only way to do this is to assume that η be small and hence derivatives are large. Given that $\theta = O(1)$ as $\zeta \rightarrow \infty$, it is essential to find appropriate scaling for f and η . On balancing the f''' , θ and $\zeta f''$ term in (15), it is found that $\eta = O(\zeta^{-1})$ and $f = O(\zeta^{-3})$ as $\zeta \rightarrow \infty$. Therefore, the following transformations may be introduced:

$$f = \zeta^{-3} \bar{f}(\eta), \quad \eta = \zeta \bar{\eta}, \quad g = \zeta^{-2} \bar{g}(\eta) \theta = \bar{\theta}(\eta) \quad (30)$$

Eqs. (15)–(18) together with the transformations given in (30) then become

$$\begin{aligned} \bar{f}''' + \bar{f}'' + \bar{\theta} - \frac{M}{(1+m^2)} \zeta^{-2} (\bar{f}' + m \bar{g}) \\ = \frac{1}{4} \zeta^{-3} \left[\bar{f}' \frac{\partial \bar{f}'}{\partial \zeta} - \bar{f}'' \frac{\partial \bar{f}}{\partial \zeta} \right] \end{aligned} \quad (31)$$

$$\begin{aligned} \bar{g}'' + \bar{g}' - \frac{M}{(1+m^2)} \zeta^{-2} (\bar{g} - m \bar{f}') \\ = \frac{1}{4} \zeta^{-3} \left[\bar{f}' \frac{\partial \bar{g}}{\partial \zeta} - \bar{g}' \frac{\partial \bar{f}}{\partial \zeta} \right] \end{aligned} \quad (32)$$

$$\frac{1}{Pr} \bar{\theta}'' + \bar{\theta}' = \frac{1}{4} \zeta^{-3} \left[\bar{f}' \frac{\partial \bar{\theta}}{\partial \zeta} - \bar{\theta}' \frac{\partial \bar{f}}{\partial \zeta} \right] \quad (33)$$

For sufficiently large ζ we expand the functions in powers of ζ^{-2} which are given below

$$\bar{f}(\zeta, \eta) = \sum_{i=0}^{\infty} \zeta^{-2i} \bar{f}_i(\eta)$$

$$\bar{g}(\zeta, \eta) = \sum_{i=0}^{\infty} \zeta^{-2i} \bar{g}_i(\eta)$$

$$\bar{\theta}(\zeta, \eta) = \sum_{i=0}^{\infty} \zeta^{-2i} \bar{\theta}_i(\eta)$$

Now we substitute the above expressions in (31)–(33) and consider the terms up to $O(\zeta^{-6})$. Thus we find the equations for zeroth order as given below:

$$\bar{f}_0''' + \bar{f}_0'' + \bar{\theta}_0 = 0 \quad (34)$$

$$\bar{g}_0'' + \bar{g}_0' = 0 \quad (35)$$

$$\frac{1}{Pr} \bar{\theta}_0'' + \bar{\theta}_0' = 0 \quad (36)$$

These equations satisfy the following boundary conditions:

$$\begin{aligned} \bar{f}(0) = \bar{f}'(0) = 0, \quad \bar{g}(0) = 0, \quad \bar{\theta}(0) = 1 \\ \bar{f}'(\infty) = \bar{g}(\infty) = \bar{\theta}(\infty) = 0 \end{aligned} \quad (37)$$

The equations of the order $O(\zeta^{-2})$ are:

$$\bar{f}_1''' + \bar{f}_1'' + \bar{\theta}_1 - \frac{M}{(1+m^2)} (\bar{f}_0' + m \bar{g}_0) = 0 \quad (38)$$

$$\bar{g}_1'' + \bar{g}_1' - \frac{M}{(1+m^2)} (\bar{g}_0 - m \bar{f}_0') = 0 \quad (39)$$

$$\frac{1}{Pr} \bar{\theta}_1'' + \bar{\theta}_1' = 0 \quad (40)$$

$$\begin{aligned} \bar{f}_1 = \bar{f}_1' = 0, \quad \bar{g}_1 = \bar{\theta}_1 = 0 \quad \text{at } \eta = 0 \\ \bar{f}_1' \rightarrow 0, \quad \bar{g}_1 \rightarrow 0, \quad \bar{\theta}_1 \rightarrow 0 \quad \text{as } \eta \rightarrow \infty \end{aligned} \quad (41)$$

The equations of the order $O(\zeta^{-4})$ are:

$$\bar{f}_2''' + \bar{f}_2'' + \bar{\theta}_2 - \frac{M}{(1+m^2)} (\bar{f}_1' + m \bar{g}_1) = 0 \quad (42)$$

$$\bar{g}_2'' + \bar{g}_2' - \frac{M}{(1+m^2)} (\bar{g}_1 - m \bar{f}_1') = 0 \quad (43)$$

$$\frac{1}{Pr} \bar{\theta}_2'' + \bar{\theta}_2' = 0 \quad (44)$$

$$\begin{aligned} \bar{f}_2 = \bar{f}_2' = 0, \quad \bar{g}_2 = \bar{\theta}_2 = 0 \quad \text{at } \eta = 0 \\ \bar{f}_2' \rightarrow 0, \quad \bar{g}_2 \rightarrow 0, \quad \bar{\theta}_2 \rightarrow 0 \quad \text{as } \eta \rightarrow \infty \end{aligned} \quad (45)$$

Finally, the equations of the order of $O(\zeta^{-6})$ are found to be:

$$\begin{aligned} \bar{f}_3''' + \bar{f}_3'' + \bar{\theta}_3 - \frac{M}{(1+m^2)} (\bar{f}_2' + m \bar{g}_2) \\ = -\frac{1}{2} (\bar{f}_0' \bar{f}_1' - \bar{f}_0'' \bar{f}_1) \end{aligned} \quad (46)$$

$$\bar{g}_3'' + \bar{g}_3' - \frac{M}{(1+m^2)} (\bar{g}_2 - m \bar{f}_2') = -\frac{1}{2} (\bar{f}_0' \bar{g}_1 - \bar{g}_0' \bar{f}_1) \quad (47)$$

$$\frac{1}{Pr} \bar{\theta}_3'' + \bar{\theta}_3' = -\frac{1}{2} (\bar{f}_0' \bar{\theta}_1 - \bar{\theta}_0' \bar{f}_1) \quad (48)$$

$$\begin{aligned} \bar{f}_3 = \bar{f}_3' = 0, \quad \bar{g}_3 = \bar{\theta}_3 = 0 \quad \text{at } \eta = 0 \\ \bar{f}_3' \rightarrow 0, \quad \bar{g}_3 \rightarrow 0, \quad \bar{\theta}_3 \rightarrow 0 \quad \text{as } \eta \rightarrow \infty \end{aligned} \quad (49)$$

The solutions of Eqs. (34)–(49) are obtained analytically, which enable us to calculate various flow parameters. The local skin-friction coefficient, $C_{fx} Gr_x^{-3/4}$, and the local rate of heat transfer in terms of the local Nusselt number coefficient, $Nu_x Gr_x^{-1/4}$, are as given below:

$$\begin{aligned} C_{fx} Gr_x^{-3/4} = \zeta^{-1} A_1 (Pr - 1) + \zeta^{-3} A_2 (Pr - 1) \\ + \zeta^{-5} (E_5 + E_1 Pr^2 + 4E_2 + E_3 (Pr + 1)^2 \\ + 4E_4 Pr^2) \end{aligned} \quad (50)$$

$$\begin{aligned} Nu_x Gr_x^{-1/4} = \zeta Pr + \zeta^{-3} ((C_3 + C_4) Pr - C_3 (Pr + 1) \\ - 2PrC_4) \end{aligned} \quad (51)$$

where

$$\begin{aligned} A_1 = \frac{1}{Pr(Pr - 1)}, \quad A_2 = B_1, \quad A_3 = \frac{B_1 M}{A_1} \\ B_1 = \frac{M}{Pr^2 (Pr - 1)^2 (1 + m^2)}, \quad B_2 = \frac{B_1 (Pr - 1)}{Pr} \\ B_3 = -B_1, \quad B_4 = \frac{B_1}{Pr} \end{aligned}$$

$$\begin{aligned}
C_3 &= \frac{B_1 Pr^2}{2(Pr+1)}, & C_4 &= -\frac{B_1}{4Pr} \\
D_2 &= \frac{A_3 M}{(1+m^2)} - \frac{Pr A_1 B_2}{2}, & D_3 &= \frac{A_1(A_2 - B_1)}{2} \\
D_4 &= A_1 A_2 - \frac{Pr A_1 B_1}{2} - \frac{A_1 B_3}{2} - C_3 \\
D_5 &= \frac{Pr A_1 B_3}{2} - \frac{A_1 A_2}{2} - C_4 \\
E_1 &= \frac{D_2}{Pr^2(Pr-1)}, & E_2 &= \frac{D_3}{4} \\
E_3 &= -\frac{D_4}{Pr(Pr+1)^2}, & E_4 &= -\frac{D_5}{4Pr^2(Pr-1)} \\
E_5 &= -Pr E_1 - 2E_2 - E_3(Pr+1) - 2Pr E_4
\end{aligned}$$

From the above solutions it can be seen that for large ζ the value of the local skin-friction,

$$C_{fx} Gr_x^{-3/4} \approx Pr/\zeta$$

and the local Nusselt number

$$Nu_x Gr_x^{-1/4} \approx Pr \zeta$$

These asymptotic solutions thus obtained for different values of the pertinent parameters have been compared with finite difference solutions, discussed below, through Table 1 and Figs. 2 and 3.

3.3. Local nonsimilarity method (LNS)

The local nonsimilarity method was developed by Sparrow and Yu [38] and has been developed and applied by many investigators, for example Minkowycz and Sparrow [35] and Chen [39] and Hossain [40], to solve various nonsimilar boundary layer problems. This method embodies two essential features. First the nonsimilar solution at any specific streamwise location is found (i.e. each solution is locally autonomous). Second, the local solutions are found from differential equations. These equations can be solved numerically by well-established techniques, such as forward integration (e.g. a Runge–Kutta scheme) in conjunction with a shooting procedure to determine the unknown boundary conditions at the wall. The method also allows some degree of self-checking for accuracy of the numerical results.

In the local nonsimilarity method, all the terms in the transformed conservation equations are retained, with the ζ derivatives distinguished by the introduction of the new functions $f_1 = \partial f / \partial \zeta$, $g_1 = \partial g / \partial \zeta$ and $\theta_1 = \partial \theta / \partial \zeta$. These represent three additional unknown functions, therefore it is necessary to deduce three further equations to determine f_1 , g_1 and θ_1 . This is accomplished by creating subsidiary equations by differentiation of the transformed conservation equations and boundary conditions (i.e., f, g, θ system of equations) with respect to ζ . The subsidiary equations for f_1 , g_1 and θ_1 contain terms $\partial f_1 / \partial \zeta$, $\partial g_1 / \partial \zeta$, $\partial \theta_1 / \partial \zeta$, and their η derivatives. If these terms are neglected, the system of equations for f, g, θ, f_1, g_1 and θ_1 reduces to a system of ordinary differential equations that

provides locally autonomous solutions in the streamwise direction. This form of the local nonsimilarity method is referred to as the second-level of truncation, because approximations are made by dropping terms in the second level equation (the f, g, θ equations being the first level equations).

The procedure as described above in the formulation of the local nonsimilarity method can result in a large number of ordinary differential equations that may require simultaneous solution. For example, at the second level of truncation there will be six equations involving $f, g, \theta, f_1, g_1, \theta_1$. It is expected that the accuracy of the local nonsimilarity method results will depend upon the truncation level. Below we give only the equations valid up to the second level of truncation:

$$\begin{aligned}
f''' + \frac{3}{4} f f'' - \frac{1}{2} f'^2 + \zeta f'' + \theta - \frac{M}{(1+m^2)}(f' + mg) \\
= \frac{1}{4} \zeta [f_1' f' - f'' f_1]
\end{aligned} \quad (52)$$

$$\begin{aligned}
g'' + \frac{3}{4} f g' - \frac{1}{2} f' g + \zeta g' - \frac{M}{(1+m^2)}(g - m f') \\
= \frac{1}{4} \zeta [f' g_1 - g' f_1]
\end{aligned} \quad (53)$$

$$\frac{1}{Pr} \theta'' + \frac{3}{4} f \theta' + \zeta \theta' = \frac{1}{4} \zeta [f' \theta_1 - \theta' f_1] \quad (54)$$

$$\begin{aligned}
f_1''' + \frac{3}{4} f f_1'' - \frac{5}{4} f' f_1' + f_1 f'' + f'' \\
+ \zeta f_1'' + \theta_1 - \frac{M}{(1+m^2)}(f' + mg) \\
= \frac{1}{4} \zeta [f_1'^2 - f_1'' f_1]
\end{aligned} \quad (55)$$

$$\begin{aligned}
g_1'' + \frac{3}{4} f g_1' - \frac{3}{4} f' g_1 + f_1 g' - \frac{1}{2} f_1' g + g' \\
+ \zeta g_1' - \frac{M}{(1+m^2)}(g_1 - m f_1') \\
= \frac{1}{4} \zeta [g_1 f_1' - g_1' f_1]
\end{aligned} \quad (56)$$

$$\begin{aligned}
\frac{1}{Pr} \theta_1'' + \frac{3}{4} f \theta_1' + f_1 \theta_1' - \frac{1}{4} f' \theta_1 + \theta_1' + \zeta \theta_1' \\
= \frac{1}{4} \zeta [f' \theta_1 - \theta_1' f_1]
\end{aligned} \quad (57)$$

$$\begin{aligned}
f(\zeta, 0) = f'(\zeta, 0) = g(\zeta, 0) = 0, & \quad \theta(\zeta, 0) = 1 \\
f_1(\zeta, 0) = f_1'(\zeta, 0) = g_1(\zeta, 0) = 0, & \quad \theta_1(\zeta, 0) = 0 \\
f'(\zeta, \infty) = f_1'(\zeta, \infty) = g(\zeta, \infty) = g_1(\zeta, \infty) \\
= \theta(\zeta, \infty) = \theta_2(\zeta, \infty) = 0
\end{aligned} \quad (58)$$

It can be seen that Eqs. (52)–(58) form a coupled nonlinear system of ordinary differential equations taking ζ as a parameter. Eqs. (52)–(58) are solved numerically, employing here the Nachtsheim–Swigert iteration technique. Here, solutions of these equations are obtained, up to the second level of truncation, for values of M equal to 0.5, $m = 100.0$ and for Prandtl

Table 1
Comparison of present authors with Markin [13]

	Merkin [13]	Present
f_0''	0.642	0.6421
θ_0	0.567	0.5671
f_1''	0.040	0.0397
θ_1'	0.483	0.4827

number equal to 0.7 and with ζ values starting from 0.0 to 80.0. Results for surface heat transfer is given in Table 1. Comparison between the nonsimilarity solutions and the finite difference solutions shows that consideration of the above equations up to the second level of truncation is sufficient for the present case.

3.4. Finite difference solutions (FDS) for entire ζ regime

For entire ζ regime we now proceed to integrate the locally nonsimilar partial differential Eqs. (9)–(11) subject to the boundary conditions (12) using the implicit finite difference method. The partial differential Eqs. (9)–(11) are first converted into a system of first order equations with dependent variables $u(\zeta, \eta)$, $v(\zeta, \eta)$, $p(\zeta, \eta)$ and $q(\zeta, \eta)$ as follows:

$$f' = U \quad (59)$$

$$u' = V \quad (60)$$

$$g' = P \quad (61)$$

$$\theta' = Q \quad (62)$$

Eqs. (9)–(12) then take the forms:

$$\begin{aligned} V' + p_1 f V - p_2 U^2 + \zeta V + \theta - p_4(U + mg) \\ = p_3 \zeta \left[U \frac{\partial U}{\partial \zeta} - V \frac{\partial f}{\partial \zeta} \right] \end{aligned} \quad (63)$$

$$\begin{aligned} P' + p_1 f P - p_2 U g + \zeta P - p_4(g - mU) \\ = p_3 \zeta \left[U \frac{\partial g}{\partial \zeta} - P \frac{\partial f}{\partial \zeta} \right] \end{aligned} \quad (64)$$

$$\frac{1}{Pr} Q' + p_1 f Q + \zeta Q = p_3 \zeta \left[U \frac{\partial \theta}{\partial \zeta} - Q \frac{\partial f}{\partial \zeta} \right] \quad (65)$$

$$\begin{aligned} f = U = g = 0, \quad \theta = 1 \quad \text{at } \eta = 0 \\ u = 0, \quad g = h = 0 \quad \text{as } \eta \rightarrow \infty \end{aligned} \quad (66)$$

where

$$p_1 = \frac{3}{4}, \quad p_2 = \frac{1}{2}, \quad p_3 = \frac{1}{4}, \quad p_4 = \frac{M}{(1+m^2)} \quad (67)$$

We now consider the net rectangle on the (ζ, η) plane and denote the net points by

$$\zeta^0 = 0, \quad \zeta^i = \zeta^{i-1} + k_i, \quad i = 1, 2, \dots, N \quad (68)$$

$$\eta_0 = 0, \quad \eta_j = \eta_{j-1} + l_j, \quad j = 1, 2, \dots, J$$

$$\eta_J = \eta_\infty \quad (69)$$

Here i and j index points on the (ζ, η) plane, and k_i and l_j give the variable mesh width.

We approximate the quantities (f, u, v, g, p, h, q) at points (ζ^i, η_j) of the net by $(f_j^i, u_j^i, v_j^i, g_j^i, p_j^i, h_j^i, q_j^i)$ which we call the net function. The notation m_j^i is also employed for any net function quantities midway between the net points as follows:

$$\zeta^{i-1/2} = \frac{1}{2}(\zeta^i + \zeta^{i-1}) \quad (70)$$

$$\eta_{j-1/2} = \frac{1}{2}(\eta_j + \eta_{j-1}) \quad (71)$$

$$m_j^{i-1/2} = \frac{1}{2}(m_j^i + m_j^{i-1}) \quad (72)$$

$$m_{j-1/2}^i = \frac{1}{2}(m_j^i + m_{j-1}^i) \quad (73)$$

We now write the difference equations that are to approximate Eqs. (59)–(62) by considering one mesh rectangle. We start by writing the finite difference approximation to Eqs. (59)–(62) using central difference quotients and average about the mid point $(\zeta^i, \eta_{j-1/2})$ to obtain:

$$\frac{f_j^i - f_{j-1}^i}{h_j} = U_{j-1/2}^i \quad (74)$$

$$\frac{U_j^i + U_{j-1}^i}{h_j} = V_{j-1/2}^i \quad (75)$$

$$\frac{g_j^i - g_{j-1}^i}{h_j} = P_{j-1/2}^i \quad (76)$$

$$\frac{\theta_j^i - \theta_{j-1}^i}{h_j} = Q_{j-1/2}^i \quad (77)$$

Similarly Eqs. (63)–(66) can be expressed in finite difference form, by approximating the functions and their derivatives by central differences about the midpoints $(\zeta^{i-1/2}, \eta_{j-1/2})$, giving the following nonlinear difference equations:

$$\begin{aligned} h_j^{-1}(V_j^i - V_{j-1}^i) + \alpha_1(fV)_{j-1/2}^i - \alpha_2(U^2)_{j-1/2}^i \\ + \zeta_{j-1/2}^i V_{j-1/2}^i + \theta_{j-1/2}^i - p_4(U_{j-1/2}^i + mg_{j-1/2}^i) \\ + \alpha(V_{j-1/2}^{i-1} f_{j-1/2}^i - f_{j-1/2}^{i-1} V_{j-1/2}^i) = R_{j-1/2}^{i-1} \end{aligned} \quad (78)$$

$$\begin{aligned} h_j^{-1}(P_j^i - P_{j-1}^i) + \alpha_1(fP)_{j-1/2}^i - \alpha_2(UG)_{j-1/2}^i \\ + \zeta_{j-1/2}^i P_{j-1/2}^i - p_4(g_{j-1/2}^i - mU_{j-1/2}^i) \\ + \alpha[U_{j-1/2}^{i-1} g_{j-1/2}^i - U_{j-1/2}^i g_{j-1/2}^{i-1} + P_{j-1/2}^i f_{j-1/2}^{i-1} \\ - P_{j-1/2}^{i-1} f_{j-1/2}^i] = X_{j-1/2}^{i-1} \end{aligned} \quad (79)$$

$$\begin{aligned} \frac{1}{Pr}[h_j^{-1}(Q_j^i - Q_{j-1}^i)] + \alpha_1(fQ)_{j-1/2}^i + \zeta_{j-1/2}^i Q_{j-1/2}^i \\ + \alpha[U_{j-1/2}^{i-1} \theta_{j-1/2}^i - U_{j-1/2}^i \theta_{j-1/2}^{i-1} \\ + Q_{j-1/2}^{i-1} f_{j-1/2}^i - Q_{j-1/2}^i f_{j-1/2}^{i-1}] = T_{j-1/2}^{i-1} \end{aligned} \quad (80)$$

where

$$R_{j-1/2}^{i-1} = -L_{j-1/2}^{i-1} + \alpha[(fV)_{j-1/2}^{i-1} - (U^2)_{j-1/2}^{i-1}] \quad (81)$$

$$L_{j-1/2}^{i-1} = [h_j^{-1}(V_j - V_{j-1}) + p_1(fV)_{j-1/2} - p_2(U^2)_{j-1/2} + \zeta_{j-1/2}(V_{j-1/2}) + \theta_{j-1/2} - p_4(U_{j-1/2}) + mg_{j-1/2}]^{i-1} \quad (82)$$

$$X_{j-1/2}^{i-1} = -Y_{j-1/2}^{i-1} + \alpha[(fP)_{j-1/2}^{i-1} - (Ug)_{j-1/2}^{i-1}] \quad (83)$$

$$Y_{j-1/2}^{i-1} = [h_j^{-1}(P_j - P_{j-1}) + p_1(fP)_{j-1/2} - p_2(Ug)_{j-1/2} + \zeta_{j-1/2}P_{j-1/2} - p_4(g_{j-1/2} - mU_{j-1/2})]^{i-1} \quad (84)$$

$$T_{j-1/2}^{i-1} = -M_{j-1/2}^{i-1} + \alpha[(fQ)_{j-1/2}^{i-1} - (U\theta)_{j-1/2}^{i-1}] \quad (85)$$

$$M_{j-1/2}^{i-1} = \left[\frac{1}{Pr} h_j^{-1}(Q_j - Q_{j-1}) + p_1(fQ)_{j-1/2} + \zeta_{j-1/2}Q_{j-1/2} \right]^{i-1} \quad (86)$$

$$\alpha = p_3 k_i^{-1} \zeta^{i-1}, \quad \alpha_1 = p_1^i + \alpha, \quad \alpha_2 = p_2^i + \alpha \quad (87)$$

The wall and the edge boundary conditions are:

$$f_0^i = 0, \quad U_0^i = 0, \quad g_0^i = 0, \quad \theta_0^i = 1 \\ U_j^i = 0, \quad g_j^i = \theta_j^i = 0 \quad (88)$$

If we assume $f_j^{i-1}, u_j^{i-1}, v_j^{i-1}, g_j^{i-1}, p_j^{i-1}, \theta_j^{i-1}, q_j^{i-1}$ to be known for $0 \leq j \leq J$, Eqs. (78)–(80) are a system of $7J + 7$ nonlinear algebraic equations for $7J + 7$ unknowns ($f_j^i, u_j^i, v_j^i, g_j^i, p_j^i, \theta_j^i, q_j^{i-1}$), $j = 1, 2, \dots, J$. These nonlinear system of algebraic equations are linearized by means of Newton's method and solved in a very efficient manner by using the Keller-box method (see Cebeci and Bardshaw [38]). For a given ζ , the iterative procedure was stopped to give the final velocity and temperature distribution when the difference in computing these functions in the next procedure becomes less than 10^{-6} , i.e., $|\delta f^k| \leq 10^{-6}$, where the superscript k denotes iteration number. For these computations, a nonuniform grid in the η direction has been used, with $\eta_j = \sinh((j-1)/a)$, where $j = 1, 2, 3, \dots, J$. Here, $J = 351$ and $a = 100$ had been chosen in order to obtain quick convergence and thus save computational time and space. It should be mentioned that convergent solutions at every ζ stations had been found within three iterations only. In the present integration scheme, values of ζ are increased with the increment $\Delta\zeta = 0.05$ until the asymptotic values for the skin-friction, heat transfer and mass transfer were reached for every variation of the pertinent parameters, such as m and M for $Pr = 0.01, 0.1$ and 0.7 .

4. Results and discussion

In the present paper, we have investigated the problem of natural convection boundary layer flow of an electrically conducting, viscous and incompressible fluid near a semi-infinite heated permeable vertical flat plate. The fluid motion is subjected to a uniform applied magnetic field normal to the plate. Hall current effects are taken into consideration. After certain transformation, numerical solutions are obtained by using: the finite difference method and local nonsimilarity method for all

Table 2
Comparison of present authors with Cobble [21]

M	Cobble [21]		Present	
	$f''(0)$	$\theta'(0)$	$f''(0)$	$\theta'(0)$
0.0	0.67464	−0.50716	0.67355	−0.50717
0.1	0.66163	−0.50084	0.66063	−0.50099
0.2	0.64934	−0.49474	0.64829	−0.49499

ξ , the perturbation method for small ξ and, the asymptotic method for large ξ , of the momentum and energy equations. The results are presented in terms of the local skin-friction, local Nusselt number, velocity profile and temperature profile. The comparison between the finite difference solutions to the solutions by other methods is found to be excellent.

The similarity solutions of the present problem obtained by Cobble [23] for the influence of magnetic field strength on the local skin friction and heat flux at the wall are shown in Table 2. The corresponding values obtained by the present authors also inserted in Table 2 and found an excellent agreement between the two results.

The numerical values of local skin-friction, $C_{fx} Gr_x^{-3/4}$ and local Nusselt number, $Nu_x Gr_x^{-1/4}$, against the transpiration parameter ξ , obtained by the methods mentioned above for $Pr = 0.7$, magnetic parameter $M = 0.5$, Hall parameter $m = 100.0$ are shown in Table 3 against values of ζ in $[0, 300]$. The comparison shows that the solutions for small and large ζ are in excellent agreement with those of the finite difference solutions as well as the local nonsimilarity solutions. From this Table it is also observed that an increase in the value of the transpiration parameter ζ , the local skin-friction start to decrease slowly but local Nusselt number start to increase firstly.

Computed values of local skin-friction coefficient, $C_{fx} \times Gr_x^{-3/4} (= f''(\zeta, 0))$, and local Nusselt number coefficient, $Nu_x Gr_x^{-1/4} (= \theta'(\zeta, 0))$, against transpiration parameter ζ for different values of Prandtl number Pr ($= 0.01, 0.1, 0.7$) are displayed in Figs. 2(a) and 2(b), respectively. From these Figures we see excellent agreement between the results obtained for smaller and larger values of the local transpiration parameter ζ , with those obtained by the finite difference method. Fig. 2(a) shows that an increase in the value of Prandtl number, Pr , leads to a decrease in the value of local skin-friction coefficient, $f''(\zeta, 0)$. Large Prandtl number corresponds to a large momentum boundary layer thickness relative to the thermal boundary layer thickness. Therefore, as Pr increases, the velocity gradient within the boundary layer decreases and thermal gradient increases. From Fig. 2(b) it can be observed that the value of local Nusselt number coefficient, $\theta'(\zeta, 0)$, increases with the increasing values of Prandtl number. It can also be observed from the Fig. 2(a) that for each value of Pr there exist local maxima in the local skin-friction coefficient, $f''(\zeta, 0)$, within the boundary layer region. For $Pr = 0.01, 0.1$ and 0.7 , the maximum values occur at $\zeta = 8.97, 3.10$ and 0.56 , and they are $3.15818, 1.91717$ and 0.95248 , respectively.

The effects of varying values of the magnetic parameter, M ($= 0.0, 0.5, 0.75$), on $C_{fx} Gr_x^{-3/4}$ and $Nu_x Gr_x^{-1/4}$, against tran-

Table 3

Numerical values of local skin friction and Nusselt number coefficients against the transpiration parameter ζ while $Pr = 0.7$, $M = 0.5$, $m = 100.0$ obtained by different methods

ζ	$C_{fx}/Gr_x^{3/4}$			$Nu_x/Gr_x^{1/4}$		
	FDS	ESS & ASS	LNS	FDS	ESS & ASS	LNS
0.00	0.9584	0.9577 s	0.9567	0.3532	0.3535 s	0.3542
0.40	1.0053	1.0027 s	1.0030	0.5051	0.5056 s	0.5055
0.60	1.0098	1.0076 s	1.0072	0.5926	0.5932 s	0.5939
1.00	0.9802	0.9765 s	0.9709	0.7900	0.7907 s	0.7922
2.00	0.7086	0.7562 s	0.7065	1.4028	1.4050 s	1.4051
2.50	0.5717	0.7611 s	0.5730	1.7494	1.7546 s	1.7499
5.00	0.2857		0.2860	3.5000		3.4997
20.00	0.0714		0.0714	13.9995		14.0000
40.00	0.0357		0.0357	27.9985		28.0000
50.00	0.0285	0.0286 a	0.0286	34.9981	35.0000 a	34.9300
60.00	0.0238	0.0238 a	0.0238	41.9977	42.0000 a	42.0000
70.00	0.0204	0.0204 a	0.0205	48.9974	49.0000 a	48.8600
80.00	0.0178	0.0179 a	0.0180	55.9971	56.0000 a	55.5800

Here 's' stands for series solutions and 'a' stands for asymptotic solutions.

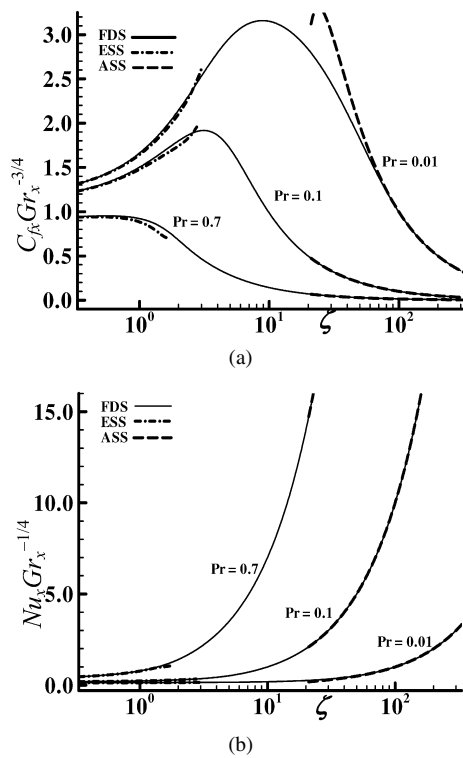


Fig. 2. (a) Local skin friction and (b) Local Nusselt number for different values of Prandtl number against Transpiration parameter ζ for $M = 0.5$, $m = 2.0$.

spiration parameter ζ are displayed in Fig. 3(a) and Table 4 respectively for the case $Pr = 0.01$ and $m = 2.0$. From these figures we see excellent agreement between the results obtained for low and high values of the local transpiration parameter ζ , with those obtained by the finite difference method for any transpiration parameter ζ . Fig. 3(a) and Table 4 also show that when magnetic parameter increases, then both the local skin-friction coefficient, $f''(\zeta, 0)$, and local Nusselt number coefficient, $\theta'(\zeta, 0)$, decreases. Magnetic field therefore decreases frictional effects and provides cooling effect. It can also be observed from the Fig. 3(a) that for each value of M there exists

Table 4

Local Nusselt number for different values of magnetic parameter against Transpiration parameter ζ for $Pr = 0.01$, $m = 2.0$

ζ	$M = 0$	$M = 0.5$	$M = 0.75$
0.00	0.13652	0.13613	0.13586
0.20	0.13739	0.13705	0.13679
0.40	0.13843	0.13808	0.13786
0.60	0.13938	0.13903	0.13881
0.80	0.14027	0.13994	0.13973
1.00	0.14119	0.14086	0.14065
2.01	0.14575	0.14551	0.14537
4.02	0.15511	0.15500	0.15494
5.04	0.16022	0.16015	0.16011
10.02	0.18846	0.18845	0.18844
20.01	0.25589	0.25589	0.25589
40.31	0.42261	0.42262	0.42262
82.01	0.82164	0.82164	0.82164
100.17	1.00214	1.00214	1.00214
145.02	1.45015	1.45017	1.45017
201.71	2.01718	2.01714	2.01714

local maxima in the local skin-friction near the leading edge and then its value decreases to the asymptotic value as ζ increases. For $M = 0.0, 0.5$ and 0.75 , the maximum values occur at $\zeta = 8.19, 8.79$ and 9.34 , and they are $3.25029, 3.15821$ and 3.11198 , respectively.

The effect of varying Hall parameter, $m (= 0.0, 2.0, 100.0)$, on the local skin-friction, $C_{fx} Gr_x^{-3/4}$, and the local Nusselt number, $Nu_x/Gr_x^{1/4}$ against transpiration parameter ζ are displayed in Fig. 3(b) and Table 5 respectively for the case $Pr = 0.01$ and $M = 0.5$. From these figures we see excellent agreement between the results obtained for low and high values of the local transpiration parameter ζ , with those obtained by the finite difference method for any transpiration parameter ζ . Fig. 3(b) and Table 5 also show that when hall parameter increases, then both the local skin-friction and local Nusselt number increases. It can also be observed from Fig. 3(b) that for each value of m there exists a local maximum in the local skin-friction near the leading edge and then its value decreases to the asymptotic value as ζ increases. For $m = 0.0, 2.0$

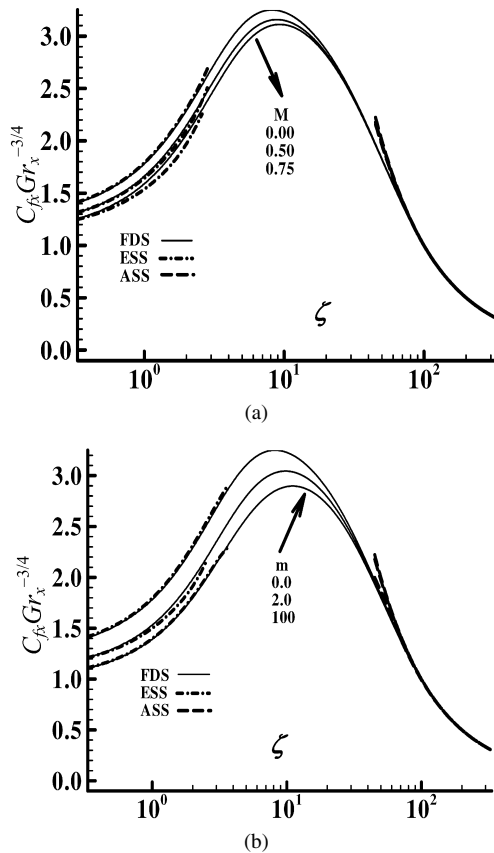


Fig. 3. Local skin friction for different values of (a) magnetic parameter against transpiration parameter ζ for $Pr = 0.01$, $m = 2.0$ and (b) for different values of Hall parameter against ξ for $M = 0.5$, $Pr = 0.01$.

Table 5
Local Nusselt number for different values of Hall parameter against Transpiration parameter ξ for $M = 0.5$, $Pr = 0.01$

ζ	$m = 0.0$	$m = 2.0$	$m = 100$
0.00	0.13519	0.13567	0.13652
0.20	0.13600	0.13659	0.13744
0.40	0.13724	0.13769	0.13843
0.60	0.13819	0.13863	0.13937
0.80	0.13911	0.13955	0.14027
1.00	0.14002	0.14047	0.14119
2.01	0.14486	0.14522	0.14574
4.02	0.15465	0.15485	0.15511
5.04	0.15991	0.16005	0.16022
10.02	0.18840	0.18843	0.18846
20.01	0.25588	0.25589	0.25589
40.31	0.42262	0.42262	0.42259
82.01	0.82164	0.82164	0.82166
100.17	1.00214	1.00214	1.00215
180.70	1.80699	1.80701	1.80699

and 100.0, the maximum values occur at $\zeta = 10.97$, 9.72 and 8.19 , and they are 2.89780 , 3.04494 and 3.24975 , respectively.

In all of the above figures the dashed curves represent the solutions obtained, respectively, for the low and high values of the local transpiration parameter, ζ and the solid curve represents the finite difference method for any values of the local transpiration parameter, ζ .

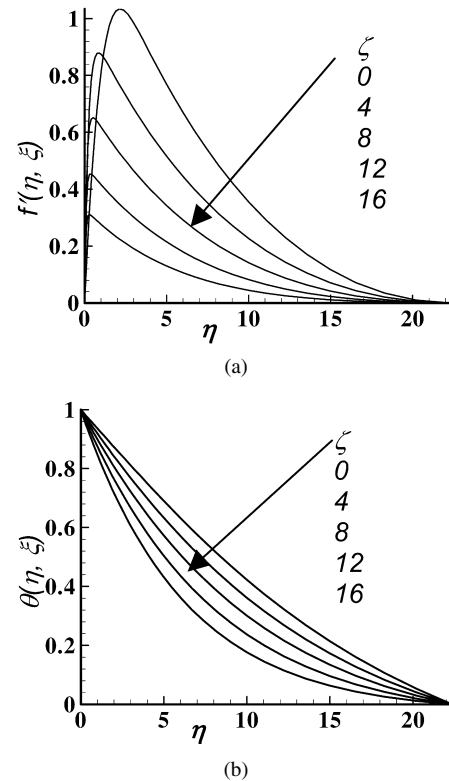


Fig. 4. (a) Velocity profile and (b) Temperature profile for different values of transpiration parameter ζ while Prandtl number $Pr = 0.01$, magnetic parameter $M = 0.5$, and Hall parameter $m = 2.0$.

Now attention is given to the effect of local transpiration parameter, ζ on the dimensionless velocity profile, $f'(\xi, \eta)$ and the dimensionless temperature profile, $\theta(\xi, \eta)$, in the flow field, obtained by the finite difference method. The numerical values of dimensionless velocity and temperature distribution are depicted graphically in Figs. 4(a) and 4(b), respectively, against η for values of $\xi = 0.0, 4.0, 8.0, 12.0, 16.0$ while $Pr = 0.01$. From Fig. 4(a) it can be seen that the velocity profiles decrease with the increase in transpiration parameter ζ . It can also be seen that at each value of ζ there exist local maximum values in velocity profile in the boundary layer region. These maximum values are 1.03398 , 0.87917 , 0.65148 , 0.45351 and 0.31162 at $(\eta, \xi) = (2.13, 0.0)$; $(0.89, 4.0)$; $(0.52, 8.0)$, $(0.41, 12.0)$ and $(0.30, 16.0)$, respectively. Fig. 4(b) shows that the temperature profiles decrease as the transpiration parameter ζ increase. We further observe that the momentum and thermal boundary layer thickness decreases with the increasing values of ζ . This is because of the suction effects of the surface mass transfer.

5. Conclusions

In this paper we have sought to determine how the presence of magnetic and hall parameter affects the natural convection boundary-layer flow from a uniformly heated permeable surface with uniform mass flux of fluid. Solutions of the governing local nonsimilarity equations are obtained by three distinct methodologies, namely, the extended series solution method for lower values of ζ , the asymptotic solutions for higher val-

ues of ζ , the local nonsimilarity method with third level of truncation and the finite difference method for all $\zeta \in [0, \infty]$. The detailed effect of varying m and M are complicated and selected results have been presented for a Prandtl number of 0.01. Detailed numerical calculations have been carried out and presented in terms of local Nusselt number and skin friction. In general it is seen that the asymptotic solutions for small and large values of the transpiration parameter are in excellent agreement with the finite difference as well as the local similarity solutions.

From the above investigations we may also draw the following conclusions:

- An increase in the value of m serves to increase both the local skin-friction and local Nusselt number.
- An increase in the value of M serves to decrease both the local skin-friction and local Nusselt number.
- Increase in the value of the transpiration parameter, ζ , leads to decrease in the momentum and thermal boundary layer thickness.

References

- [1] K.R. Sing, T.G. Cowling, Thermal convection in magnetohydrodynamic boundary layers, *J. Mech. Appl. Math.* 16 (1963) 1–5.
- [2] E.M. Sparrow, R.D. Cess, The Effect of a magnetic field on free convection heat transfer, *Int. J. Heat Mass Transfer* 3 (1961) 267–274.
- [3] A.S. Gupta, Flow of an electrically conducting fluid past a porous flat plate in the presence of a transverse magnetic field, *J. Appl. Math. Phys. (ZAMP)* 11 (1960) 43–50.
- [4] N. Riley, Magnetohydrodynamic free convection, *J. Fluid Mech.* 18 (1964) 267–277.
- [5] H.K. Kuiken, Magnetohydrodynamic free convection in a strong cross-field, *J. Fluid Mech.* 40 (1970) 21–38.
- [6] G. Wilks, Magnetohydrodynamic free convection about a semi-infinite vertical plate in a strong cross-field, *J. Appl. Math. Phys.* 27 (1976) 621–631.
- [7] M.A. Hossain, K.C.A. Alam, D.A.S. Rees, MHD free and forced convection boundary layer flow along a vertical porous plate, *Appl. Mech. Engrg.* 2 (1997) 33–51.
- [8] M.A. Hossain, I. Pop, M. Ahmed, MHD free convection flow from an isothermal plate inclined at a small angle to the horizontal, *J. Theor. Appl. Fluid Mech.* 1 (1996) 194–207.
- [9] M.A. Hossain, Viscous and joule heating on MHD free-convection flow with variable plate temperature, *Int. J. Heat Mass Transfer* 35 (1992) 3485–3487.
- [10] E.M. Elbashbeshy, Heat and mass transfer along a vertical plate with variable surface temperature and concentration in the presence of the magnetic field, *Int. J. Engrg. Sci.* 34 (1997) 515–522.
- [11] R. Eichhorn, The effect of mass transfer on free convection, *ASME J. Heat Transfer* 82 (1960) 260–263.
- [12] E.M. Sparrow, R.D. Cess, Free convection with blowing and suction, *Int. J. Heat Mass Transfer* 823 (1961) 387.
- [13] J.H. Merkin, Free convection with blowing and suction, *Int. J. Heat Mass Transfer* 154 (1961) 989–999.
- [14] J.H. Merkin, The effect of blowing and suction on free convection boundary layer, *Int. J. Heat Mass Transfer* 18 (1975) 237–244.
- [15] P.G. Perikh, R. Moffat, W. Kays, D. Bershader, Free convection over a vertical porous plate with transpiration, *Int. J. Heat Mass Transfer* 17 (1974) 1465–1474.
- [16] J.P. Hartnett, E.R.G. Eckert, Mass transfer cooling in a laminar boundary layer with constant fluid properties, *ASME J. Heat Transfer* 79 (1975) 247–254.
- [17] E.M. Sparrow, J.B. Starr, The transpiration cooling flat plate with various thermal and velocity boundary condition, *Int. J. Heat Mass Transfer* 9 (1966) 508–510.
- [18] T.T. Kao, Laminar incompressible forced convection along a flat plate with arbitrary suction or injection at the wall, *Trans. ASME J. Heat Transfer* 97 (1975) 484–486.
- [19] T.T. Kao, Locally non-similar solution for laminar free convection adjacent to a vertical wall, *Trans. ASME J. Heat Transfer* 98 (1976) 321–322.
- [20] M. Vedhanayagam, R.A. Altenkirch, R. Echhorn, A transformation of the boundary layer equation for free convection flow past a vertical flat plate with arbitrary blowing and wall temperature variation, *Int. J. Heat Mass Transfer* 23 (1980) 1236–1288.
- [21] H.T. Lin, W.S. Yu, Free convection on horizontal plate with blowing and suction, *ASME J. Heat Transfer* 110 (1988) 793–796.
- [22] M.A. Hossain, S.K. Das, I. Pop, Heat transfer response of MHD free convection flow along a vertical flat plate to surface temperature oscillations, *Int. J. Non-Linear Mech.* 33 (1998) 541–553.
- [23] M.H. Cobble, Free convection with mass transfer under the influence of a magnetic field, *Nonlinear Analysis* 3 (1979) 135–143.
- [24] V.M. Soundalgekar, M. Singh, H.S. Takhar, MHD free convection past a semi-infinite vertical plate with suction and injection, *Nonlinear Analysis* 7 (1983) 941–944.
- [25] H. Sato, The Hall effect in the viscous flow of ionized gas between two parallel plates under transverse magnetic field, *J. Phys. Soc. Japan* 16 (1961) 1427.
- [26] T. Yamanishi, Hall effect in the viscous flow of ionized gas through straight channels, in: 17th Annual Meeting, Phys. Soc. Japan 5 (1962) 29.
- [27] A. Sherman, G.W. Sutton, *Magnetohydrodynamics*, Evanston, Illinois, 1961, 173 pp.
- [28] M. Katagiri, The effect Hall currents on the viscous flow magnetohydrodynamic boundary layer flow past a semi-infinite flat plate, *J. Phys. Soc. Japan* 27 (1969) 1051.
- [29] A.S. Gupta, Hydrodynamic flow past a porous flat plate with Hall effects, *Acta Mechanica* 22 (1975) 281.
- [30] Nanigopal Datta, Bijoyshingha Mazumder, Hall effects on hydrodynamic free convection flow past an infinite porous flat plate, *J. Math. Phys. Sci.* 10 (1975) 59.
- [31] I. Pop, V.M. Soundalgekar, Effects of Hall current on hydromagnetic flow near a porous plate, *Acta Mechanica* 20 (1974) 315–318.
- [32] I. Pop, T. Watanabe, Hall effect on magnetohydrodynamic free convection about a semi-infinite vertical flat plate, *Int. J. Eng. Sci.* 32 (1994) 1903.
- [33] Aboeldahab, M. Emad, Elbarbary, M.E. Elsayed, Hall current effect on magnetohydrodynamic free convection flow past a semi-infinite plate with mass transfer, *Int. J. Eng. Sci.* 39 (2001) 1641.
- [34] H.B. Keller, Numerical methods in boundary layer theory, *Annual Rev. Fluid. Mech.* 10 (1978) 417–433.
- [35] W.J. Minkowycz, E.M. Sparrow, Numerical solution scheme for local nonsimilarity boundary layer analysis, *Numerical Heat Transfer* 1 (1978) 69–85.
- [36] J.C. Butcher, Implicit Runge–Kutta process, *Math. Comp.* 18 (1964) 50–55.
- [37] P.R. Nachtsheim, P. Swigert, Satisfaction of the asymptotic boundary conditions in numerical solution of the system of nonlinear equations of boundary layer type, NASA TND-3004, 1965.
- [38] E.M. Sparrow, H.S. Yu, Local nonsimilarity thermal boundary layer solutions, *Trans. ASME J. Heat Transfer* 93 (1971) 328–334.
- [39] T.S. Chen, Parabolic system: local nonsimilarity method, in: W.J. Minkowycz, E.M. Sparrow, G.E. Schneider, R.H. Pletcher (Eds.), *Handbook of Numerical Heat Transfer*, Wiley, New York, 1988.
- [40] M.A. Hossain, Effect of transpiration on combined heat and mass transfer in mixed convection along a vertical plate, *Int. J. Energy Res.* 16 (1992) 761–769.